THE *UNIVERSITY of* EDINBURGH

Edinburgh Research Explorer

Identification of two molecular subtypes in canine mast cell tumours through gene expression profiling

OPEN ACCESS

RESEARCH ARTICLE

Identification of two molecular subtypes in canine mast cell tumours through gene expression profiling

Lidia H. Pulz[1,2]*, Camila N. Barra[1,2], Pamela A. Alexandre[1], Greice C. Huete[1], Karine G. Cadrobbi[1], Adriana T. Nishiya[3], Silvio Henrique de Freitas[1], Heidge Fukumasu[1], Ricardo F. Strefezzi[1]

1 Department of Veterinary Medicine, Faculty of Animal Science and Food Engineering, University of São Paulo, Pirassununga, SP, Brazil, 2 Department of Pathology, Faculty of Veterinary Medicine and Animal Science- FMVZ, University of Sao Paulo, São Paulo, SP, Brazil, 3 Veterinary Hospital Anhembi Morumbi, R. Conselheiro Lafaiete, São Paulo—SP, Anhembi Morumbi University, São Paulo, SP, Brazil

* hplidia@gmail.com

Abstract

Mast cell tumours (MCTs) are common neoplasms in dogs and are usually regarded as potentially malignant. Several studies have attempted to identify biomarkers to better predict biological behaviours for this tumour. The aim of this study was to identify pathways connected to clinical and histopathological malignancies, shorter survival times, and poor prognoses associated with MCTs. We performed genome-wide gene expression analyses on tissues obtained from 15 dogs with single MCTs, and identified two distinct tumour subtypes —high-risk and low-risk—associated with differences in histological grades, survival times, Ki67 indices, and occurrence of death due the disease. Comparative analyses of RNA sequence profiles revealed 71 genes that were differentially expressed between high- and low-risk MCTs. In addition to these analyses, we also examined gene co-expression networks to explore the biological functions of the identified genes. The network construction revealed 63 gene modules, of which 4 were significantly associated with the more aggressive tumour group. Two of the gene modules positively correlated with high-risk MCTs were also associated with cell proliferation and extracellular matrix-related terms. At the top of the extracellular matrix module category, genes with functions directly related to those of cancer-associated fibroblasts (CAFs) were identified. Immunohistochemical analyses also revealed a greater number of CAFs in high-risk MCTs. This study provides a method for the molecular characterisation of canine MCTs into two distinct subtypes. Our data indicate that proliferation pathways are significantly involved in malignant tumour behaviours, which are known to be relevant for the induction and maintenance of MCTs. Finally, animals presenting high-risk MCTs overexpress genes associated with the extracellular matrix that can be robustly linked to CAF functions. We suggest that CAFs in the MCT stroma contribute to cancer progression.

Introduction

Canine mast cell tumours (MCTs) are malignant neoplasms composed of atypical mast cells that are characterised by high infiltration capacity and metastatic potential [1, 2]. It is one of the most commonly diagnosed neoplasms in dogs, accounting for 16–21% of cutaneous tumours [3–7]. Since the biological behaviours of MCTs are highly variable, a better understanding of the development and progression, as well as the identification of new prognostic indicators, can help in treating the diseased animals [8].

Like most tumours in animals, canine MCTs are classified based on their histological appearances, which presumably reflect degree of cell differentiation. Besides this classification, prediction of biological behaviours in MCTs could be complemented by additional methods based on histochemical and immunohistochemical prognostic markers [9–12]. However, as in human neoplasms, abundant evidence suggests the presence of unrecognised, relevant subclasses of tumours with respect to their underlying molecular phenotypes and prognoses [13]. Clinically, it is also apparent that histologically identical tumours can behave very differently [14].

The transcriptomes of canine cancers have been investigated mainly by cDNA microarrays in mammary tumours [15, 16], osteosarcomas [17, 18, 19], hemangiosarcomas [20, 21], lymphomas [22, 23], histiocytic sarcomas [24], mast cell tumours [25, 26], and melanoma cell lines [27]. Compared to microarrays, next generation RNA sequencing (RNA-seq) is a more powerful technique, allowing the investigation of gene expression data at a whole-transcriptome level with unprecedented sensitivity and accuracy [28]. Recent investigations of canine tumours with RNA-seq have been carried out in B-cell lymphomas [29], mammary carcinomas [30], squamous cell carcinomas of the head and neck [31], bladder cancers [32], and hemangiosarcomas [33].

In this study, we aimed to identify molecular pathways associated with MCT behaviour using differential expression and co-expression network analyses with RNA-seq-based transcriptomics data from canine MCTs samples. To the best of our knowledge, this is the first study to characterise MCTs using network methods.

Materials and methods

Canine tissue samples

Since only animals with single lesions were included in this study, a total of 15 cutaneous MCTs from 15 dogs were utilised. Fresh-frozen and formalin-fixed paraffin-embedded (FFPE) tissue sections of spontaneous canine MCTs were obtained from the Veterinary Hospitals of the School of Veterinary Medicine and Animal Science of the University of São Paulo, Methodist University of São Paulo and the Veterinary Clinic Provet. Samples were acquired from routine cases that were treated by wide surgical resectioning. All experiments were approved by "Ethics Committee for the use of animals" of the School of Veterinary Medicine and Animal Science of the University of São Paulo #2893/2013 and consent for the use of foreskin tissue was provided by the legal guardians of all tissue donors in this study.

All tumours were chosen based on the following inclusion criteria: 1) confirmed histological diagnosis of canine cutaneous MCT; 2) treatment with surgical excision without neoadjuvant chemotherapy (no radiation or chemotherapy before or at the time of tumour removal); 3) availability of follow-up data.

Each tumour was evaluated according to a two-tier grading system into low-grade (grade 1) or high-grade (grade 2) of malignancy [34] by the same veterinary pathologist (R. F. Strefezzi), who was not supplied with any information about the cases. The choice of this histopathological

grading criteria eliminates the ambiguity of intermediate grade MCTs and is more accurate in predicting the biological behaviour of this tumour [9, 34].

Follow-up data collection began from the day of first contact, and continued for at least 180 days post-surgery and included details of age, sex, breed, location of the lesions, time to relapse, overall survival and *causa mortis*, when applicable. Overall survival was defined as the interval between surgical excision and last follow-up day or death by any cause. At the end of the study, deaths unrelated to MCT were censored. Nine dogs (60%) received adjuvant chemotherapy. The treatment protocols included combinations of vinblastine, prednisone, and lomustine.

Ki67 immunohistochemical staining

FFPE tissues were sectioned into 5 μm-thick sections, deparaffinised in xylene, rehydrated in graded ethanol, and rinsed in distilled water. Endogenous peroxidases were blocked by incubating sections in 3% hydrogen peroxide for 5 m. Antigen retrieval was performed by incubating the sections in citrate buffer (pH 6.0) in a pressure cooker for 2 m and cooled for 20 m. All slides were rinsed with 0.05 M phosphate buffered saline (PBS, pH 7.6) with 0.01% Tween 20. The slides were subsequently incubated with mouse monoclonal anti-Ki67 primary antibodies (MIB1; Dako Cytomation Carpinteria, CA) at a dilution of 1:50, in a moist chamber at 4 °C for 16 h (overnight). Following this, slides were incubated with secondary antibodies (Code K4068, ADVANCE^{TM} HRP Link, anti-mouse and anti-rabbit secondary antibodies, Dako, Carpinteria, CA) for 25 m and the reaction was amplified with Advance HRP Enzyme Polymer (Code K4068, ADVANCE^{TM} HRP Enzyme, antibodies polymerised with horseradish peroxidase, Dako Cytomation Carpinteria, CA). The reactions were visualised with 3,4-diaminobenzidine (Liquid DAB + Substrate Chromogen System, Dako Cytomation Carpinteria, CA) and counterstained with Mayer's haematoxylin.

For the negative control, the primary antibody was replaced with a normal mouse IgG at the same concentration as the primary antibody. The basal layer of the epidermis served as an internal positive control for Ki67.

Ki67 index

Histological images were evaluated distant from the deep and lateral margins of the tumour mass. For each lesion, a total of five high power fields (HPF) (400x magnification) were selected from areas with the highest percentage of labelled mast cells ("hot spots") at low magnification (100x magnification). To determine the percentage of proliferating cells (Ki67 index), we counted the number of mast cells showing positive and negative immunostaining for Ki67 in the chosen fields per captured image using the ImageJ software; a minimum of 200 cells for each section were counted. We determined the average percentage of positive mast cells in five fields without prior knowledge of the clinical outcome.

Definition of high-risk and low-risk MCTs

We used four criteria to divide MCT samples into low- or high-risk groups: histological grade, survival time, Ki67 index and death due the disease. The tumours were graded histologically with a two-tier system (low-grade or grade 1 and high-grade or grade 2). Each parameter received a score, which was added to the histological grade to obtain a combined score or score of malignancy.

For survival time, a score of 1 was designated to animals that remained alive for > 365 days; a score of 2, to those surviving for $180 \geq 365$ days; and a score of 3, for animals with survival times of < 180 days.

Scores to evaluate the Ki67 indices of MCT samples were assigned as follows: a score of 1 was assigned to lesions that showed less than 3% immunoreactive cells; a score of 2 was assigned to lesions that showed 3% to 7% immunoreactive cells; and a score of 3 was assigned to lesions that displayed more than 7% of Ki67-positive cells [35].

Finally, one of the most important biological characteristics to be considered in the study of cancers is their capacity to cause death of the patient. A score to quantify occurrence of death in the studied animals was created by assigning a grade of 0 to all animals that remained alive at the end of the study period, as well as to all censored animals, whereas a score of 3 was assigned to dogs that died due the tumour.

Lesions with a total score of 5 or below were classified as "low-risk" MCTs (samples S02, S03, S05, S06, S07, S08, S09, S11, S13, S14 and S15) and those with a score of 6 or more were defined as "high-risk" MCTs (samples S01, S04, S10 and S12).

Immunohistochemical staining for αSMA

We evaluated the expression of αSMA in stromal fibroblasts of 44 canine MCTs using immunohistochemistry in FFPE tissues, with a mouse monoclonal antibody (Clone HHF35; Dako Denmark A/S, Glostrup, Denmark). For negative controls, the primary antibody was replaced with normal rabbit or normal mouse IgG at the same concentration as the primary antibody.

All animals from which lesion samples were obtained for the study met the following criteria: 1) all were treated with extensive surgery; 2) none were subjected to neoadjuvant chemotherapy; and 3) follow-up data for at least 180 days was available. Lesions were obtained from routine cases and confirmed as MCTs by histopathology. The Veterinary Hospitals of the School of Veterinary Medicine and Animal Science of the University of São Paulo, Methodist University of São Paulo and the Veterinary Clinic Provet submitted the samples for the analyses.

The same criteria applied for the MCTs analysed by RNA-seq were used to divide the tumours subjected to immunohistochemical analysis into low- and high-risk groups: histological grade, survival time, Ki67 index and death due to disease. The term "low-risk" was attributed to cases with a score lower than 6 and high-risk for tumours with a total score equal to or greater than 6.

The number of positive fibroblasts were counted in five HPFs (400x magnification), using the ImageJ software. Fields were selected from areas with the highest percentage of labelled cells ("hot spots") at low magnification (100x magnification); the score was calculated from the sum of cells counted in five "hot spots" fields.

Statistical analysis

Ki67 index values of 44 MCT samples divided into high- and low-risk groups were compared using the Mann-Whitney U test. The number of fibroblasts testing positive for αSMA immunostaining was also compared between the low- and high-risk groups using the Mann-Whitney U test. The data were analysed with GraphPad Prism (version 4.02 for Windows, GraphPad Software, GraphPad Software Inc.) with the significance level set at 5%.

RNA extraction

Total RNA from each of the 15 fresh-frozen tissue samples were extracted using the RNeasy Mini Kit (Cat No./ID: 74104, Qiagen, Crawley, West Sussex, UK). All samples satisfied the criteria of a nucleic acid 260/280 ratio of approximately 2.0 and were subjected to further analyses. RNA quality was assessed using capillary gel electrophoresis on a BioAnalyzer system (Agilent Technologies Inc., Santa Clara, CA) with RNA 6000 Nano Labchips (Agilent

Technologies Inc., Santa Clara, CA, EUA) according to the manufacturer's instructions. Only samples exhibiting minimal degradation as evidenced by RNA Integrity Number (RIN) ≥ 7.0 were used.

RNA-seq data analysis

Sequencing was conducted using the Illumina platform (Illumina Inc., San Diego, CA), following the protocols provided by the manufacturer. Total RNA from 15 samples were converted into Illumina sequencing libraries using the TruSeq RNA Sample Preparation Kit in accordance with TruSeq RNA Sample Preparation v2 Guide (Illumina, USA, 2012, Part # 15026495 Rev. D). PolyA RNA was enriched from 1 μg of total RNA using oligo dT-coated magnetic beads, following which, the enriched RNA was fragmented and used for cDNA synthesis. The cDNA was fragmented, blunt-ended, ligated to bar-coded adaptors, and amplified using 15 cycles of PCR. Final library size distribution was validated through quantitative polymerase chain reaction (qPCR) using an Agilent 2100 Bioanalyzer with a KAPA Library Quantification kit (KAPA Biosystems, Foster City, USA). Adapter-ligated cDNA fragment libraries were run on Illumina HiSeq 2500 equipment using the TruSeq PE Cluster Kit and the TruSeq SBS Kit (2x100 bp). An average of 28.4 million PE 100-bp reads were sequenced per sample.

Sequencing quality was evaluated using the FastQC software (http://www.bioinformatics. babraham.ac.uk/projects/fastqc/) and due to its high quality, no filter was applied prior to alignment. Read pairs were aligned to the dog reference genome (CanFam3.1) with *TopHat2/ Bowtie2* (tophat.cbcb.umd.edu), allowing two mismatches per read. The sequence alignment map (SAM) files were filtered using Samtools [36] to remove secondary alignments, PCR duplicates, and low-quality alignments. Following this, read counts for each gene was estimated using HTSeq [37]. Gene expression was estimated as counts per million (CPM) and genes which presented at least 1 CPM in at least 4 samples were retained for DE analysis.

DE analysis was performed using the EdgeR package, which is based on negative binomial distributions, in the R environment [38]. Only transcripts with adjusted P-values (P_{aj}) ≤ 0.05 e logFC $\geq |2|$ were considered to be differentially expressed. To ensure that the differentially expressed genes were sufficient to differentiate between the 2 groups, a hierarchical clustering analysis was performed. Over-/under-expressed genes in canine MCTs were identified on a heatmap.

Co-expression analysis

Co-expression analysis was used to generate a transcriptional network to investigate associations between gene modules and malignancy grades of MCTs. The analysis was performed using the WGCNA (Weighted Correlation Network Analysis) package in the R environment [39]. From the total of 13,948 genes which passed quality control, only the 6000 most-connected genes were selected due to computational limitations; furthermore, genes with low connectivity were not considered since they are likely to contribute little to the network [40].

Connectivity was calculated as the sum of correlations between one gene and all other genes in the network. To identify modules, a matrix was first generated by calculating Pearson's correlation coefficients between all genes and raising it to a power β (soft threshold) of 11. Following this, a topological overlap measure (TOM) was calculated by assigning values between 0 and 1 to each pair of genes based on the number of shared neighbours; this was then used to generate a clustering tree whose branches were identified for cutting using the dynamic tree-cutting algorithm [41]. Modules containing a minimum of 30 genes were detected and assigned to colour names. Pearson's correlation coefficients were used again to measure correlations between modules' expression profiles (module eigengenes) and the

malignancy scores described earlier. Modules with significant correlations ($p < 0.1$) were considered biologically relevant and used for further analysis.

Functional enrichment analysis

A web-server interactive software tool, GOrilla, was used to identify GO terms enriched in both the differentially expressed genes and co-expression modules associated with tumour malignancy; this was done using a hypergeometric distribution with corrections for false positive rate or false discovery rate (FDR). Genes were converted to their human orthologues to obtain the best functional detail available. Only expressed genes were used as background and terms were considered significant only if $P_{aj} \leq 0.05$.

Results

Clinical and histopathological data and Ki67 index values

A total of 15 dogs diagnosed with MCT were included in this study. The median age at diagnosis was 10 years (mean = 9.7 years, range = 3–15 years) and 41.2% of the patients were male. The most common breeds represented in our sample were Labrador Retrievers (5 dogs), Golden Retrievers (3 dogs) and Pit bulls (2 dogs). The remaining dogs in the sample were a poodle, dachshund, Cocker Spaniel, pug and mongrel. The most frequent locations of the MCTs were in the extremities (40% in the limbs and tail) and trunk (33.3%), followed by the abdomen and inguinal regions (13.3% each). A summary of the descriptions of the canine population is shown in Table 1.

Histopathological analyses of the MCTs were performed according to the classification system described by Patnaik et al. (1984) [42] and 4 lesions were defined as grade I (26.7%), 10 as grade II (66.7%) and 1 as grade III (6.7%). The tumours were also graded using a two-tier histological system proposed by Kiupel et al. (2011) [34], and 13 (86.7%) MCTs were classified as low-grade while only 2 (13.3%) were classified as having a high grade of malignancy.

Three dogs (S04, S10 and S12) in our sample died due to MCT aggressiveness, which caused a local recurrence of MCTs with new tumour development after surgical removal or disseminated metastases. The MCTs from all the three animals that died were graded as 'intermediate' according to the criteria of Patnaik et al. (1984) [42], and only one was diagnosed with MCT of high grade of malignancy by the two-tier histological system. One dog died due to unrelated causes and the remaining 12 cases were alive at the end of the study. The minimum follow-up period post-surgery was 190 days (median = 296 days, range = 101–1095 days) (Table 1).

The Ki67 index was determined by the percentage of neoplastic mast cells exhibiting a positive nuclear signal to anti-Ki67 antibodies. Ki67 scores ranged from 0.30–23.41% (mean = 5.7 ± 5.84%). The Ki67 scores for MCTs from the dogs that died due to tumour aggressiveness were 23.4%, 15.5% and 2.11%. (Table 1). The figures representing the different Ki67 scores are in the Supporting information (S1 Fig).

Classification of samples as high- or low-risk MCTs

The categorisation of malignancy in the MCTs was based on clinical and histopathological features. We established individual scores for measures of survival time, proliferation index, and death due the disease. Each of these scores was added to the histological grade assigned to obtain a score of malignancy (Table 2). This numerical scale allowed us to divide all MCT cases into two groups: higher scores indicated high risk of malignancy in tumours (samples S01, S04, S10 and S12), whereas lower scores indicated low risk of malignancy (samples S02, S03, S05, S06, S07, S08, S09, S11, S13, S14 and S15).

Table 1. Summary of clinical and histopathological data with their respective identification number of RNA-seq.

RNA-SEQ ID	BREED	AGE YEARS	GENDER	TUMOUR LOCATION	FOLLOW-UP (DAYS)	STATUS	PATNAIK ET AL. 1984 GRADE SYSTEM	TWO-TIER GRADING SYSTEM[a]	KI67 INDEX
S01	Dachshund	10	Male	Limbs and tail	658	CS	3	2	7.95%
S02	Labrador	11	Female	Trunk	480	LA	1	1	2.92%
S03	Poodle	15	Female	Trunk	466	LA	1	1	2.36%
S04	Golden Retriever	7	Female	Limbs and tail	308	DT	2	1	23.41%
S05	Pug	9	Female	Limbs and tail	587	LA	2	1	5.28%
S06	Pitbull	10	Female	Abdomen	254	LA	2	1	3.65%
S07	Labrador	11	Female	Trunk	364	LA	2	1	4.87%
S08	Cocker	13	Female	Trunk	283	LA	2	1	1.88%
S09	Labrador	9	Male	Limbs and tail	390	LA	2	1	3.8%
S10	Labrador	5	Female	Limbs and tail	101	DT	2	2	15.48%
S11	Golden Retriever	3	Female	Inguinal	232	LA	2	1	0.30%
S12	Labrador	10	Male	Limbs and tail	130	DT	1	1	2.11%
S13	Golden Retriever	9	Male	Trunk	191	LA	2	1	5.21%
S14	Mixed breed	13	Male	Inguinal	1095	LA	2	1	2.89%
S15	Pitbull	11	Male	Abdomen	676	LA	1	1	3.43%

Abbreviations: ID: identification number; LA: live animals; CS: censored (deaths unrelated to MCT); DT: death related to mast cell tumour.

[a] Kiupel et al. (2011)

https://doi.org/10.1371/journal.pone.0217343.t001

Canine mast cell tumour transcriptome

The number of paired end (PE) reads sequenced per sample ranged from 22,885,802 to 32,305,518 (an average of 28,404,278 PE reads were generated per sample). These sequences were mapped to the canine reference genome (canFam3.1) with a mean alignment rate of 83%, with a minimum alignment of 77.7% and maximum alignment of 86.4%. On average, the analyses revealed multiple alignments in 11% of multiple and discordant alignments in 2% of the reads. The remaining 79% of the reads were concordant alignments. Data per sample can be seen in Supporting Information (S1 Table).

Differentially expressed genes in high- and low-risk MCTs

Comparisons of transcriptome profiles between high- and low-risk MCTs revealed 71 differentially expressed (DE) genes ($P_{aj} \leq 0.05$) (Fig 1). Of these, 68 were upregulated in the high-risk group while 3 genes were downregulated (Fig 1). A list of the differentially expressed genes with their respective descriptions is available in Table 3.

Co-expression analysis

A total of 63 modules were identified when the 6000 most-connected genes from the 15 samples were used for the analysis. Genes that are highly interconnected within the network (modules) are expected to be involved in the same pathways or in roles with related biological

Table 2. Scoring of mast cell tumours.

RNA-SEQ ID	TWO-TIER GRADING SYSTEM [a]	FOLLOW-UP SCORE	STATUS SCORE	KI67 SCORE	MALIGNANCY SCORE
S01	2	1	0	3	6[b]
S02	1	1	0	1	3
S03	1	1	0	1	3
S04	1	2	3	3	9[b]
S05	1	1	0	2	4
S06	1	2	0	2	5
S07	1	2	0	2	5
S08	1	2	0	1	4
S09	1	1	0	2	4
S10	2	3	3	3	11[b]
S11	1	2	0	1	4
S12	1	3	3	1	8[b]
S13	1	2	0	2	5
S14	1	1	0	1	3
S15	1	1	0	2	4

Assignment of a score for each characteristic considered: histological grade, survival time, Ki67 index and death due the disease. The mixed score (malignancy score) method was determined from these four characteristics, which together gave a numeric value for each tumour.

Abbreviations: ID: identification number

[a]Kiupel et al. (2011)

[b]Malignancy Score $\geq$ 6 = high-risk MCT

functions. The correlation analysis between module eigengene values and malignancy scores resulted in the identification of four significant modules ($P < 0.1$) (Fig 2).

Two modules, *Palevioletred3* ($r = -0.46$, $P = 0.09$) and *Floralwhite* ($r = -0.45$, $P = 0.09$), are negatively correlated with malignancy scores, whereas the other two modules, *Darkorange2* ($r = 0.51$, $P = 0.05$) and *Darkorange* ($r = 0.45$, $P = 0.09$), were positively correlated with malignancy scores (Fig 2). The *Palevioletred3* module included 43 unique genes (S2 Table) in Supporting Information and the *Floralwhite* module included 54 genes (S2 Table). The *Darkorange* module included 85 unique genes (S2 Table) and the *Darkorange2* module with 53 genes (S2 Table) in Supporting Information.

Functional enrichment analysis

The functional enrichment analysis of all 71 DE genes indicated that these genes were connected to immune/inflammatory responses, mitochondrial activity, and extracellular region ($P_{aj} \leq 0.05$); most of them were found to be up-regulated in the high-risk group. Considering biological processes, there was an enrichment related to response to biotic stimulus ($P = 1.28 \times 10^{-10}$, 17/71), chemotaxis ($P = 1.37 \times 10^{-9}$, 12/71), response to lipopolysaccharide ($P = 6.77 \times 10^{-9}$, 11/71), immune response ($P = 7.33 \times 10^{-9}$, 16/71) and cytokine-mediated signaling pathway ($P = 8.32 \times 10^{-9}$, 13/71). When molecular functions were analysed, the enriched gene ontology (GO) terms included oxido-reductase activity ($P = 5.97^{-11}$, 7/71), mono-oxygenase activity ($P = 8.26^{-9}$, 7/71) and G-protein coupled receptor binding ($P = 9.61^{-7}$, 8/71). Interestingly, when cellular components were included in the analysis, genes related to the extracellular region were also enriched ($P = 9.65^{-10}$, 22/71).
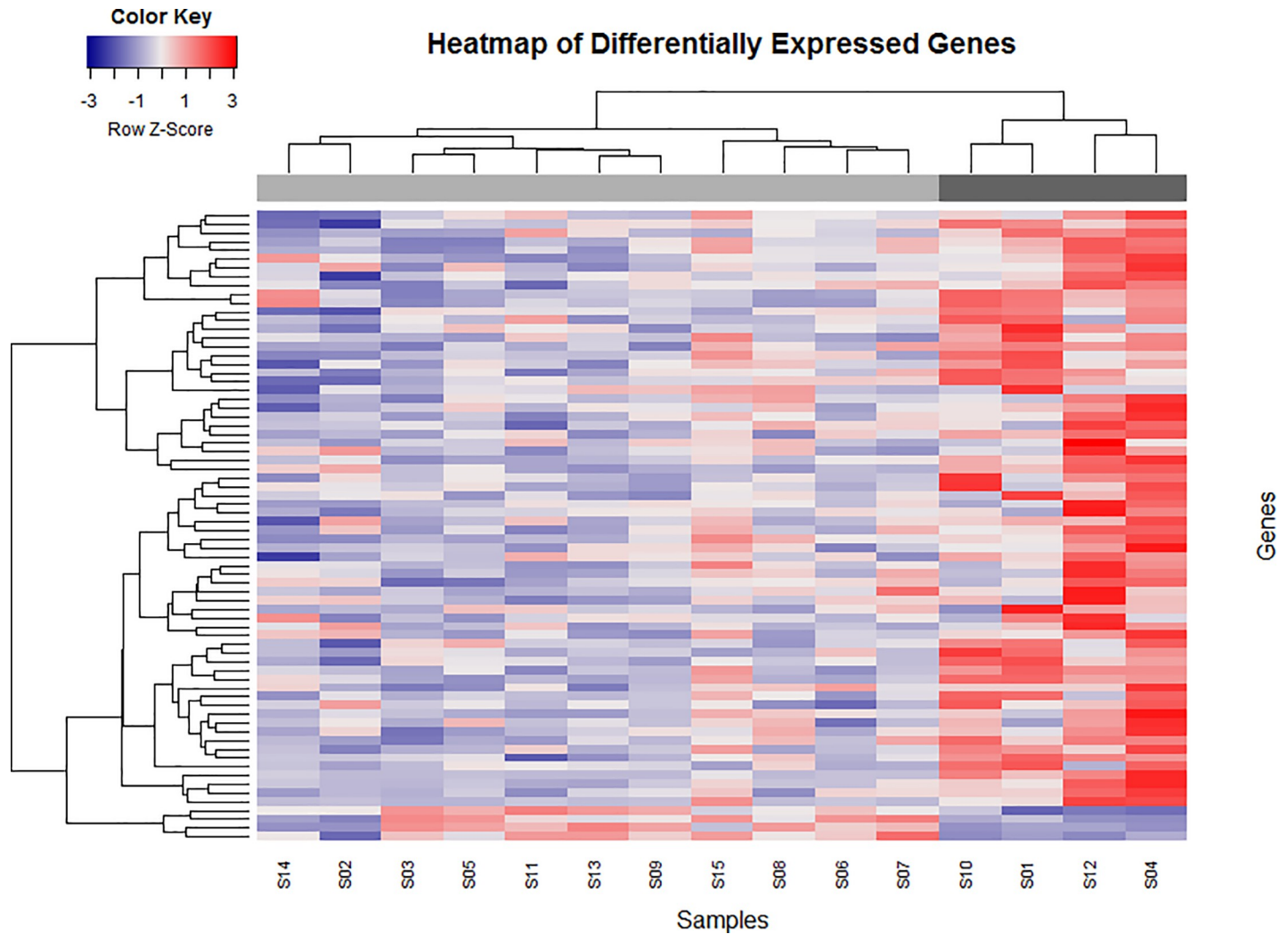
Fig 1. Hierarchical clustering of 15 dog samples based on a subset of 71 differentially expressed genes. A total of 13,948 genes are represented in a heat map. Colour intensity was normalised to log10 (fragments per kilobase of transcript per million mapped reads + 1). Increasing red intensity indicates increased gene expression and increasing blue intensity indicates decreased gene expression, as shown in the scale bar. Statistically significant differences in gene expression ($p < 0.05$) define two molecular subtypes of canine MCTs—high-risk (n = 4) and low-risk MCTs (n = 11). According to the differential gene expression profile, samples were clustered separately and arranged from the low-risk group (left/light grey bar) to the high-risk group (right/ dark grey bar).

https://doi.org/10.1371/journal.pone.0217343.g001

A new functional enrichment analysis to test for co-expression was carried out for each significant module. This analysis showed that only those modules positively correlated with MCT risk scores (*Darkorange2* and *Darkorange*) presented significant enrichment in GO ($P_{aj} \le 0.05$).

The *Darkorange2* module (53 genes) is involved mostly in biological processes related to positive regulation of cell proliferation. The most representative terms in this module included 'cell cycle process' (P = 3.08 x 10^{-17}), 'mitotic cell cycle process' (P = 9.16 x 10^{-13}), 'regulation of chromosome segregation' (P = 1.18 x 10^{-11}) and 'regulation of cell cycle' (P = 1.55 x 10^{-10}) (Fig 3A). Corroborating this result, the enriched GO terms also included 'chromosomal part' (8.1 x 10^{-9}), and 'chromosome, centromeric region' (5.11 x 10^{-8}) (Fig 3B) when cellular components were included in the analysis.

Table 3. List of Differentially expressed (DE) genes between the high-risk MCTs and low-risk MCTs.

GENE NAME	DESCRIPTION	PValue	P_{aj}
MMP3	matrix metallopeptidase 3 (stromelysin 1, progelatinase)	1.17E-20	1.63E-16
CXCL8	IL8 or C-X-C Motif Chemokine Ligand 8	3.26E-17	2.27E-13
IL1B	Interleukin 1 beta	5.95E-16	2.76E-12
FMO1	flavin containing monooxygenase 1	4.96E-11	1.73E-07
CSF3R	colony stimulating factor 3 receptor	2.02E-09	5.62E-06
MAB21L1	mab-21 like 1	3.41E-09	7.93E-06
CDO1	cysteine dioxygenase type 1	7.94E-09	1.58E-05
ensembl code	-	1.01E-08	1.77E-05
GTSF1	gametocyte specific factor 1	1.19E-08	1.85E-05
WNT5A	Wnt family member 5a	1.39E-08	1.94E-05
NCAM2	neural cell adhesion molecule 2	2.62E-08	3.33E-05
IL18BP	interleukin 18 binding protein	1.86E-07	0.0002
LOC483397	interferon-induced transmembrane protein 1	2.89E-07	0.0003
IL11	interleukin 11	5.97E-07	0.0006
IL18RAP	interleukin 18 receptor accessory protein	6.50E-07	0.0006
WIF1	WNT inhibitory factor 1	7.73E-07	0.0006
MFSD2B	major facilitator superfamily domain containing 2B	7.75E-07	0.0006
EXO1	exonuclease 1	1.54E-06	0.0012
PI15	peptidase inhibitor 15	3.13E-06	0.0023
KMO	kynurenine 3-monooxygenase	4.09E-06	0.0029
COL21A1	collagen type XXI alpha 1 chain	4.45E-06	0.0030
LOC102155886/ SAA1(human)	serum amyloid A protein-like	5.79E-06	0.0037
MYRIP	myosin VIIA and Rab interacting protein	6.09E-06	0.0037
LOC476879/ SAA1 (human)	serum amyloid A protein-like	9.23E-06	0.0054
SMPDL3A	sphingomyelin phosphodiesterase acid like 3a	1.20E-05	0.0067
ensembl code	-	1.38E-05	0.0074
EDNRB	endothelin receptor type B	1.61E-05	0.0082
HTR7	5-hydroxytryptamine receptor 7	1.74E-05	0.0082
GNAZ	G protein subunit alpha z	1.76E-05	0.0082
CHGA	chromogranin A	1.73E-05	0.0082
LOC106557449	alveolar macrophage chemotactic factor-like	2.04E-05	0.0092
PGF	placental growth fator	2.25E-05	0.0098
LOC484867	docosahexaenoic acid omega-hydroxylase CYP4F3	2.82E-05	0.0119
DNM3	dynamin 3	3.10E-05	0.0127
KLHL41	kelch like family member 41	3.30E-05	0.0128
GAB3	GRB2 associated binding protein 3	3.31E-05	0.0128
FRMPD4	FERM and PDZ domain containing 4	3.62E-05	0.0136
SAMSN1	SAM domain, SH3 domain and nuclear localization signals 1	4.05E-05	0.0149
S100A9 (human)	S100 calcium binding protein A9	4.40E-05	0.0157
TNFRSF4	TNF receptor superfamily member 4	4.53E-05	0.0158
GRIK4	glutamate ionotropic receptor kainate type subunit 4	4.76E-05	0.0162
IGKV2-24 (human)	immunoglobulin kappa variable 2–24	6.52E-05	0.0216
PNMT	phenylethanolamine N-methyltransferase	6.86E-05	0.0218
SIRPA (human)	signal regulatory protein alpha	6.77E-05	0.0218
CLEC4E	C-type lectin domain family 4 member E	8.64E-05	0.0268
CSF2RA	colony stimulating factor 2 receptor alpha subunit	9.24E-05	0.0280
MUC4 (human)	mucin 4, cell surface associated	9.47E-05	0.0281

(Continued)

Table 3. (Continued)

| GENE NAME	DESCRIPTION	PValue	P_{aj}
PLAUR	plasminogen activator, urokinase receptor	0.0001	0.0289
SPP2	secreted phosphoprotein 2	0.0001	0.0289
SLAMF1	signaling lymphocytic activation molecule family member 1	0.0001	0.0289
SOCS1	suppressor of cytokine signaling 1	0.0001	0.0306
COL11A2	collagen type XI alpha 2 chain	0.0001	0.0321
CLEC5A	C-type lectin domain family 5 member A	0.0001	0.0327
IL1RN	interleukin 1 receptor antagonist	0.0001	0.0327
CTSE	cathepsin E	0.0001	0.0334
IL2RB	interleukin 2 receptor subunit beta	0.0001	0.0356
ANOS1	anosmin 1	0.0001	0.0356
CYP27B1	cytochrome P450, family 27, subfamily B, polypeptide 1	0.0002	0.0359
IDO1	indoleamine 2,3-dioxygenase 1	0.0002	0.0364
SLC4A8	solute carrier family 4 member 8	0.0002	0.0365
HJURP	Holliday junction recognition protein	0.0002	0.0365
SOD2	superoxide dismutase 2, mitochondrial	0.0002	0.0380
UCHL1	ubiquitin C-terminal hydrolase L1	0.0002	0.0380
C20orf96	chromosome 24 open reading frame, human C20orf96	0.0002	0.0404
COL27A1 (human)	collagen type XXVII alpha 1 chain	0.0002	0.0425
IL22RA2	interleukin 22 receptor subunit alpha 2	0.0002	0.0426
DDC	dopa decarboxylase	0.0002	0.0470
GPR35	G-protein coupled receptor 35-like	0.0002	0.0486
S100A8	S100 calcium binding protein A8	0.0002	0.0489
RFX8	RFX family member 8, lacking RFX DNA binding domain	0.0003	0.0498
PCSK1N	proprotein convertase subtilisin/kexin type 1 inhibitor	0.0003	0.0498

Human orthologues were used in ensembl gene ID that not found a respective gene name in canine transcriptome.

https://doi.org/10.1371/journal.pone.0217343.t003

The second module, *Darkorange* (P = 0.09), showed functional enrichment in genes associated with the extracellular matrix (ECM). The enriched terms were 'extracellular matrix organisation' (P = 1.41 x 10^{-19}), 'extracellular structure organisation' (P = 1.55 x 10^{-19}), 'collagen metabolic process' (P = 2.28 x 10^{-14}), 'multicellular organismal macromolecule metabolic process' (P = 4.32 x 10^{-14}), and 'collagen catabolic process' (P = 1.12 x 10^{-13}) (Fig 4A). When cellular components were included in the analysis, enrichment in terms related to 'extracellular matrix' (P = 2.59 x 10^{-15}), 'endoplasmic reticulum lumen' (P = 5.75 x 10^{-15}), 'collagen trimer' (P = 2.91 x 10^{-13}), and 'extracellular matrix component' (P = 7.3 x 10^{-12}) were also included in the results (Fig 4B). When molecular functions were analysed, the enriched GO terms included 'platelet-derived growth factor binding' (P = 5.04 x 10^{-8}) and 'extracellular matrix structural constituent' (P = 1.02 x 10^{-7}) (Fig 4C).

Biological validation of significant modules

Since the *Darkorange2* module expression profile yielded robust results related to cell proliferation, we proceeded to analyse the Ki67 indices of another set of 44 MCT samples. Comparison of Ki67 indices between low-risk MCTs (samples 01–22, mean = 4.16% ± 0.03%) and high-risk (samples 23–44; mean = 8.91% ± 0.05%) revealed that the percentage of proliferating cells was significantly higher in high-risk MCTs (P = 0.0044) (S2 Fig).
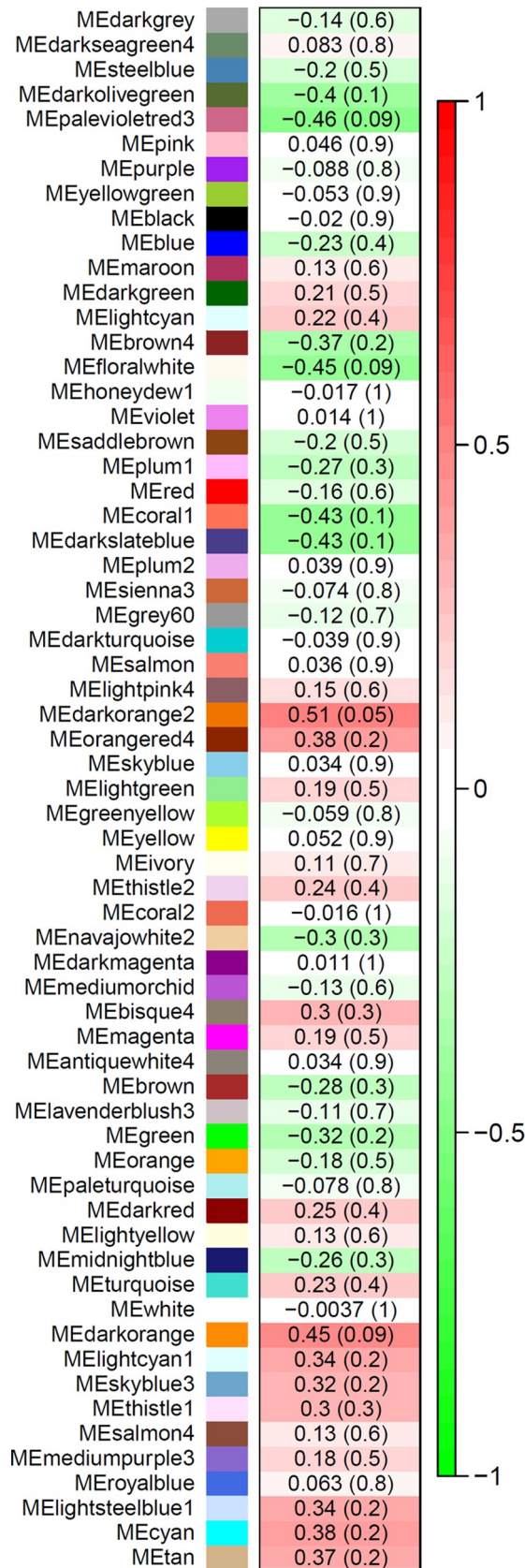
Fig 2. Correlations between module eigengene (ME) values and malignancy scores. Highly connected genes were identified in 63 modules with respective colours considering the 6000 most connected genes in all samples. The level of red intensity indicates degree of positive correlation between module expression and malignancy scores. The level of green intensity indicates the degree of negative correlation of module expression and malignancy scores. The *p*-values for correlation analyses are provided in brackets.

Since the 'extracellular matrix module' (*Darkorange* module) was significantly associated with high-risk MCTs, we further analysed samples to detect the presence of fibroblasts, one of the main components of the stroma that influences the ECM. Fibroblasts within the tumour stroma with a modified phenotype are termed 'cancer-associated fibroblasts' (CAFs) and are mostly defined based on the expression of markers such as α-smooth-muscle actin (αSMA). Immunohistochemical analyses to identify and quantify CAFs in 44 canine MCT samples revealed diffuse cytoplasmic immunostaining patterns in fibroblasts (Fig 5).

Darkorange2 module enriched GO terms associated to cell proliferattion

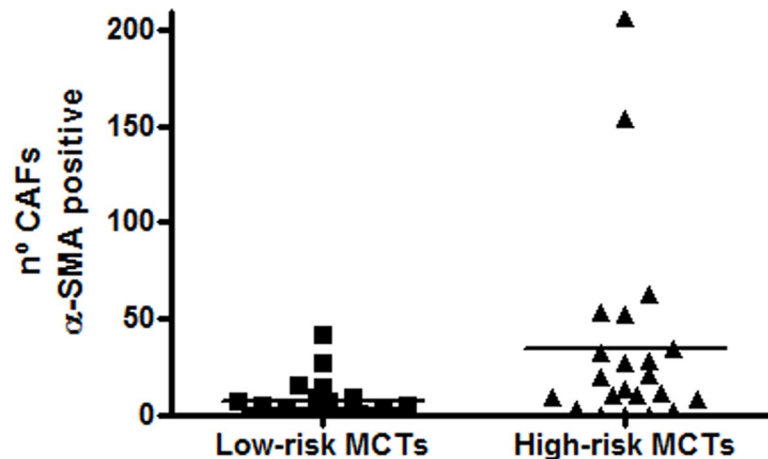**(A) Biological process**
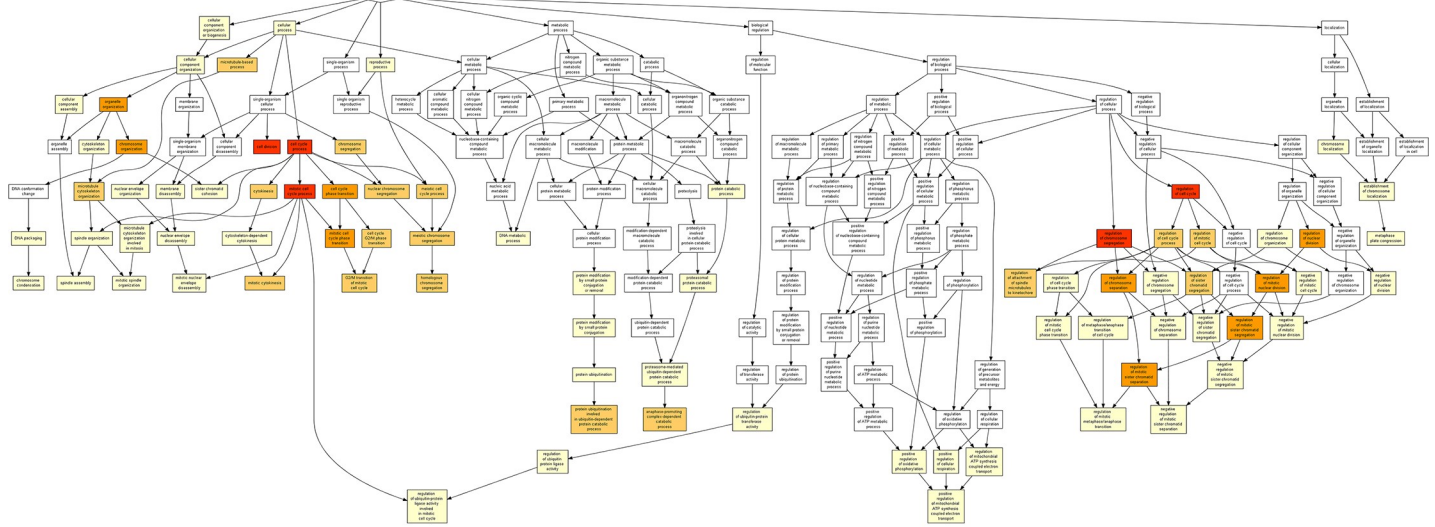
(B) Cellular Component
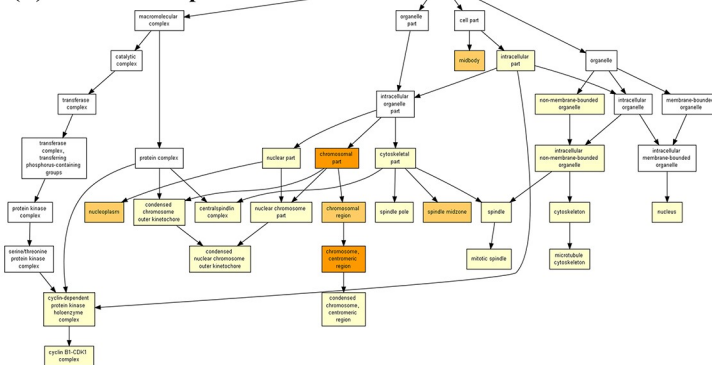
Fig 3. Enriched gene ontology (GO) terms from the *Darkorange2* module associated with cell proliferation. Colour-coded graphical representation reflecting the degree of enrichment of each (A) biological process and (B) cellular components. The higher intensity of red colour represents more significant terms.

Fig 4. Enriched gene ontology (GO) terms from the *Darkorange* module associated with the extracellular matrix (ECM). Colour-coded graphical representation reflecting the degree of enrichment of (A) biological processes, (B) cellular components and (C) molecular functions. The higher intensity of red colour represents more significant terms.

https://doi.org/10.1371/journal.pone.0217343.g004

Fig 5. Photomicrographs showing positive immunostaining for α-smooth-muscle actin (αSMA) in canine mast cell tumours (MCTs). (A) Evident stromal fibroblasts immunoexpression (400x magnification). (B) Immunostaining with anti-αSMA antibodies specifically stains the cytoplasm of cancer-associated fibroblasts (CAFs) (1000x magnification). All sections were counterstained with Harris's haematoxylin.

https://doi.org/10.1371/journal.pone.0217343.g005

Fig 6. Number of cancer-associated fibroblasts (CAFs) in mast cell tumour stroma of low-risk vs. high-risk MCTs. The number of CAFs in high-risk tumours (22 samples) (P = 0.0021, Mann-Whitney U test) was significantly higher than in low-risk tumours (22 samples).

In the 22 samples that were classified as low-risk (50%), and 22 as high-risk tumours (50%) using the malignancy score (S3 Table), CAFs were present in significantly higher numbers in MCTs classified as high-risk (P = 0.0021) (Fig 6).

Discussion

In this study, we aimed to identify the mechanisms involved in MCT progression using a transcriptomic approach. Our integrative approach, involving datasets on global gene expression profiles, co-expression analyses, functional enrichment analyses, and validation by immuno-histochemistry, revealed that high-risk MCTs are associated with genes that promote increased cellular proliferation and stimuli from the tumour stroma.

First, in a typical genome-wide expression analysis experiment, we used mRNA expression profiles to generate a large number of genes ordered in a ranked list, according to their DE in the high-risk and low-risk MCT groups. The challenge with these data was to extract biological meaning from the list obtained, since single-gene analyses may miss important roles played by whole pathways [43]. Alternatively, we performed co-expression analyses to examine our data at the level of gene sets to obtain information on significant pathways or on ontology.

Since we used proliferation index as a criterion for categorising MCT samples into high- and low-risk groups, our bioinformatics analyses show that a significant number of genes involved in providing proliferation stimuli are upregulated in high-risk MCTs. This result suggests that the molecular pathways identified in our study are biologically relevant to the phenotypes observed. Our results partially corroborate those obtained by Giantin et al. (2014) [25], who demonstrated that a different set of up-regulated genes in undifferentiated MCTs are involved in pathways regulating mitosis. An additional research with the same spontaneous canine cutaneous MCT samples also demonstrated cell cycle gene differentially regulated between aggressive and not aggressive MCTs [26]. More importantly, these results also confirm earlier results that demonstrate the importance of the Ki67 index as a prognostic indicator for MCT, independent of the histopathological grade of the disease [35, 44] and that dogs with high scores of Ki67 expression have shorter survival times [45, 46].

However, the key finding of our study was obtained from the functional enrichment analyses of transcriptomic networks involving the ECM. We must consider that RNA is extracted

from the whole MCT tissue. In addition to simply anchoring cells, it is now known that the ECM is an active and complex tissue component [47, 48]. Since fibroblasts are the most abundant cells in connective tissues and are intimately linked to the ECM, both as builders and residents, the modulatory properties of the local ECM are most apparent in fibroblast functions [49].

GO terms associated with the ECM were the most over-represented in the *Darkorange* module, and their expression levels were also positively correlated with malignancy scores. Thus, this module appears to integrate multiple ECM signatures and is likely to play an important role in the progression of MCTs. The *Darkorange* module contains 10 over-expressed collagen genes (S2 Table); as of now, it is not possible to dissociate the role of these molecules from those of the fibroblasts' matrix microenvironment. In addition, the *Darkorange* module also includes the mRNAs of Lysyl oxidase (LOX) and lysyl oxidase-like-2 (LOXL2), which are matrix enzymes that promote cross-linking of fibrillar collagen and are synthesised by fibroblasts [50]. Stromal LOX expression has been implicated in the development of the metastatic niche [51] and LOXL2 expression is also thought to play a role in promoting invasion [52–55].

Interestingly, another gene that is included in the "extracellular matrix module" is the platelet derived growth factor receptor-α (PDGFRA), a tyrosine-kinase receptor. Notably, PDGFRA expression on the cell surface is restricted to the stromal compartment in skin and tumour cells [56] and the molecule is reportedly expressed by up to 90% of stromal fibroblasts in solid tumours [57]. Local fibroblasts or fibroblast precursors stimulated by members of the PDGF or transforming growth factor beta (TGF-β) family have generally been considered to be the major source of CAFs [58]. These cells within the tumour stroma contribute structurally and functionally to the progression, growth, and spread of cancers [58–60]. CAFs in the tumour stroma acquire a modified phenotype, similar to wound healing fibroblasts, and are also known as myofibroblasts, reactive stromal fibroblasts, tumour-associated fibroblasts, or activated fibroblasts [58, 61]. Several studies highlight αSMA as an important marker for these cells [62–64].

Based on these findings, we hypothesised that high-risk tumours have an altered microenvironment influenced by CAFs. To confirm this possibility, we demonstrated by immunohistochemistry, that high-risk MCTs have higher number of CAFs in their stroma than low-risk MCTs. The importance of this subpopulation of cells in the tumour microenvironment is emphasised when taken in conjunction with the results of functional enrichment analysis of the *Darkorange* module for angiogenesis. CAFs have been shown to support tumorigenesis by stimulating angiogenesis, cancer cell proliferation, and invasion [56, 65–67].

In accordance with our results, several studies have demonstrated that higher expression levels of αSMA in tumour stromal fibroblasts is an independent prognostic marker for several human cancer types [68–70] and canine neoplasms [71]. In addition, it is interesting to note that there is an association between LOXL2 protein expression and α-SMA-positive stromal fibroblasts in diverse types of solid tumours and that LOXL2 inhibition was efficacious in inhibiting cancer growth in both primary and metastatic xenograft models [72].

Conclusions

In summary, our study indicates a set of specific genes in MCT samples that have different expression levels in high-risk and low-risk groups. An integrative analytic approach revealed that these genes are related to cellular proliferation and ECM components, mainly from stromal CAFs. While our study provides some insight into the emergent properties of CAFs, more efforts are required to validate and extend our findings.

Supporting information

S1 Fig. Ki67 immunostaining images scores in MCT samples. (A) Ki-67 reactivity in a Score 1 sample, showing less than 3% of immunoreactive cells; (B) Score 2 sample that showed 3% to 7% of specific nuclear staining in mast cells; (C) Score 3 lesion that displayed more than 7% of Ki67-positive cells.
(TIF)

S2 Fig. Ki67 index. Comparison of Ki67 indices between low-risk and high-risk MCTs.
(PDF)

S1 Table. RNA-seq data. RNA-seq data analyses with the description of each lesion detailing the percentages of alignment to the dog reference genome.
(PDF)

S2 Table. Gene co-expression networks. List of component genes of individual modules in each tab: Genes in Palevioletred3 module; Genes in Floralwhite module; Genes in Darkorange2 module; Genes in Darkorange module.
(XLSX)

S3 Table. Summary of Clinical, Histopathological and Immunohistochemical data in dogs with MCTs. Breed, age, gender, location of the lesions, follow-up time, survival data, histopathological grades, Ki67 score, quantitative analisys of CAFs with their respective malignancy score.
(PDF)

Acknowledgments

Author Contributions

Conceptualization: Adriana T. Nishiya, Silvio Henrique de Freitas, Ricardo F. Strefezzi.

Data curation: Lidia H. Pulz, Greice C. Huete, Karine G. Cadrobbi, Adriana T. Nishiya, Silvio Henrique de Freitas.

Formal analysis: Lidia H. Pulz, Heidge Fukumasu, Ricardo F. Strefezzi.

Investigation: Lidia H. Pulz, Greice C. Huete.

Methodology: Lidia H. Pulz, Camila N. Barra, Heidge Fukumasu.

Project administration: Lidia H. Pulz, Heidge Fukumasu, Ricardo F. Strefezzi.

Resources: Ricardo F. Strefezzi.

Software: Pamela A. Alexandre, Heidge Fukumasu.

Supervision: Heidge Fukumasu, Ricardo F. Strefezzi.

Validation: Pamela A. Alexandre, Karine G. Cadrobbi.

Visualization: Ricardo F. Strefezzi.

Writing – original draft: Lidia H. Pulz, Ricardo F. Strefezzi.

Writing – review & editing: Lidia H. Pulz, Heidge Fukumasu, Ricardo F. Strefezzi.

References

1.   Hottendorf GH. Pathologic report of 29 necropsies on dogs with mastocytoma. Pathol Vet Online. 1968; 5: 102–121.

2.   Blackwood L, Murphy S, Buracco P, De Vos JP, De Fornel-Thibaud P, Hirschberger J, et al. European consensus document on mast cell tumours in dogs and cats. Vet Comp Oncol. 2012; 10(3): e1–e29. https://doi.org/10.1111/j.1476-5829.2012.00341.x PMID: 22882486

3.   Cohen D, Reif JS, Brodey RS, Keiser H. Epidemiological Analysis of the Most Prevalent Sites and Types of Canine Neoplasia Observed in a Veterinary Hospital. Cancer Res. 1974; 34: 2859–2868. PMID: 4529096

4.   Priester WA. Skin Tumors in Domestic Animals. Data from 12 United States and Canadian Colleges of Veterinary Medicine. J Natl Cancer Inst. 1973; 50(2): 457–466. https://doi.org/10.1093/jnci/50.2.457 PMID: 4735678

5.   Bostock DE. Neoplasms of the skin and subcutaneous tissues in dogs and cats. Br Vet J. 1986; 142: 1–19. https://doi.org/10.1016/0007-1935(86)90002-3 PMID: 3947927

6.   London C, Seguin B. Mast cell tumors in the dog. Vet Clin North Am Small Anim Pract. 2003; 33: 473–489. PMID: 12852232

7.   Shoop SJ, Marlow S, Church DB, English K, McGreevy PD, Stell AJ, et al. Prevalence and risk factors for mast cell tumours in dogs in England. Canine Genet Epidemiol. 2015; 2(1): 1.

8.   Welle MM, Bley CR, Howard J, Rüfenacht S. Canine mast cell tumours: a review of the pathogenesis, clinical features, pathology and treatment. Vet Dermatol. 2008; 19(6): 321–339. https://doi.org/10.1111/j.1365-3164.2008.00694.x PMID: 18980632

9.   Sabattini S, Scarpa F, Berlato D, Bettini G. Histologic grading of canine mast cell tumor: Is 2 better than 3?. Vet Pathol. 2015; 52(1): 70–73. https://doi.org/10.1177/0300985814521638 PMID: 24513799

10. Vascellari M, Giantin M, Capello K, Carminato A, Morello EM, Vercelli A, et al. Expression of Ki67, BCL-2, and COX-2 in canine cutaneous mast cell tumors: association with grading and prognosis. Vet Pathol. 2013; 50(1): 110–121. https://doi.org/10.1177/0300985812447829 PMID: 22673539

11. Webster JD, Yuzbasiyan-Gurkan V, Kaneene JB, Miller R, Resau JH, Kiupel M. The Role of c-KIT in Tumorigenesis: Evaluation in Canine Cutaneous Mast Cell Tumors. Neoplasia. 2006; 8(2): 104–111. https://doi.org/10.1593/neo.05622 PMID: 16611403

12. Pulz LH, Barra CN, Kleeb SR, Xavier JG, Catão-Dias JL, Sobral RA, Fukumasu H, Strefezzi RF. Increased expression of tissue inhibitor of metalloproteinase-1 correlates with improved outcome in canine cutaneous mast cell tumours. Vet Comp Oncol. 2016; 15(2): 606–614. https://doi.org/10.1111/vco.12204 PMID: 27041588

13. Freije WA, Castro-Vargas FE, Fang Z, Horvath S, Cloughesy T, Liau LM et al. Gene expression profiling of gliomas strongly predicts survival. Cancer research. 2004; 64(18): 6503–6510. https://doi.org/10.1158/0008-5472.CAN-04-0452 PMID: 15374961

14. Mischel PS, Nelson SF, Cloughesy TF. Molecular analysis of glioblastoma: pathway profiling and its implications for patient therapy. Cancer Biol Ther. 2003; 2(3): 242–247. https://doi.org/10.4161/cbt.2.3.369 PMID: 12878856

15. Uva P, Aurisicchio L, Watters J, Loboda A, Kulkarni A, Castle J, et al. Comparative expression pathway analysis of human and canine mammary tumors. BMC Genomics. 2009; 10: 135. https://doi.org/10.1186/1471-2164-10-135 PMID: 19327144

16. Klopfleisch R, Lenze D, Hummel M, Gruber AD. Metastatic canine mammary carcinomas can be identified by a gene expression profile that partly overlaps with human breast cancer profiles. BMC Cancer. 2010; 10: 618. https://doi.org/10.1186/1471-2407-10-618 PMID: 21062462

17. Selvarajah GT, Kirpensteijn J, van Wolferen ME, Rao NAS, Fieten H, Mol JA. Gene expression profiling of canine osteosarcoma reveals genes associated with short and long survival times. Mol Cancer. 2009; 8: 72. https://doi.org/10.1186/1476-4598-8-72 PMID: 19735553

18. O'Donoghue LE, Ptitsyn AA, Kamstock DA, Siebert J, Thomas RS, Duval DL. Expression profiling in canine osteosarcoma: identification of biomarkers and pathways associated with outcome. BMC Cancer. 2010; 10: 506. https://doi.org/10.1186/1471-2407-10-506 PMID: 20860831

19. Pang LY, Gatenby EL, Kamida A, Whitelaw BA, Hupp TR, Argyle DJ. Global gene expression analysis of canine osteosarcoma stem cells reveals a novel role for COX-2 in tumour initiation. PLoS One. 2014; 9: 1–13.

20. Tamburini BA, Phang TL, Fosmire SP, Scott MC, Trapp SC, Duckett MM, et al. Gene expression profiling identifies inflammation and angiogenesis as distinguishing features of canine hemangiosarcoma. BMC Cancer. 2010; 10: 619. https://doi.org/10.1186/1471-2407-10-619 PMID: 21062482

21. Thomas R, Borst L, Rotroff D, Motsinger-Reif A, Lindblad-Toh K, Modiano JF, et al. Genomic profiling reveals extensive heterogeneity in somatic DNA copy number aberrations of canine hemangiosarcoma. Chromosom Res. 2014; 22: 305–319.

22. Frantz AM, Sarver AL, Ito D, Phang TL, Karimpour-Fard A, Scott MC, et al. Molecular Profiling Reveals Prognostically Significant Subtypes of Canine Lymphoma. Vet Pathol. 2013; 50: 1–11.

23. Mudaliar MA V, Haggart RD, Miele G, Sellar G, Tan KAL, Goodlad JR, et al. Comparative Gene Expression Profiling Identifies Common Molecular Signatures of NF-kB Activation in Canine and Human Diffuse Large B Cell Lymphoma (DLBCL). PLoS One. 2013; 8(9): e72591. https://doi.org/10.1371/journal.pone.0072591 PMID: 24023754

24. Boerkamp KM, Van der Kooij M, Van Steenbeek FG, Van Wolferen ME, Groot Koerkamp MJA, Van Leenen D, et al. Gene Expression Profiling of Histiocytic Sarcomas in a Canine Model: The Predisposed Flatcoated Retriever Dog. PLoS One. 2013; 8: e71094. https://doi.org/10.1371/journal.pone.0071094 PMID: 23936488

25. Giantin M, Granato A, Baratto C, Marconato L, Vascellari M, Morello EM, Vercelli A, Mutinelli F, Dacasto M. Global gene expression analysis of Canine cutaneous mast cell tumor: Could molecular profiling be useful for subtype classification and prognostication? PLoS One. 2014; 9(4): e95481. https://doi.org/10.1371/journal.pone.0095481 PMID: 24748173

26. Giantin M, Baratto C, Marconato L, Vascellari M, Mutinelli F, Dacasto M, et al. Transcriptomic analysis identified up-regulation of a solute carrier transporter and UDP glucuronosyltransferases in dogs with aggressive cutaneous mast cell tumours. Vet J. 2016; 212: 36–43. https://doi.org/10.1016/j.tvjl.2016.03.024 PMID: 27256023

27. Fowles JS, Denton CL, Gustafson DL. Comparative analysis of MAPK and PI3K/AKT pathway activation and inhibition in human and canine melanoma. Vet Comp Oncol. 2015; 13: 288–304. https://doi.org/10.1111/vco.12044 PMID: 23745794

28. Ozsolak F, Milos PM. RNA sequencing: advances, challenges and opportunities. Nat. Rev. Genet. 2011; 12: 87–98. https://doi.org/10.1038/nrg2934 PMID: 21191423

29. Mooney M, Bond J, Monks N, Eugster E, Cherba D, Berlinski P, et al. Comparative RNA-Seq and Microarray Analysis of Gene Expression Changes in B-Cell Lymphomas of Canis familiaris. PLoS One. 2013; 8(4): e61088. https://doi.org/10.1371/journal.pone.0061088 PMID: 23593398

30. Liu D, Xiong H, Ellis AE, Northrup NC, Rodriguez CO, O'Regan RM, et al. Molecular homology and difference between spontaneous canine mammary cancer and human breast cancer. Cancer Res. 2014; 74: 5045–5056. https://doi.org/10.1158/0008-5472.CAN-14-0392 PMID: 25082814

31. Liu D, Xiong H, Ellis AE, Northrup NC, Dobbin KK, Shin DM, et al. Canine Spontaneous Head and Neck Squamous Cell Carcinomas Represent Their Human Counterparts at the Molecular Level. PLoS Genet. 2015; 11: 1–19.

32. Ramsey SA, Xu T, Goodall C, Rhodes AC, Kashyap A, He J, et al. Cross-Species Analysis of the Canine and Human Bladder Cancer Transcriptome and Exome. Genes, Chromosom. Cancer. 2017; 56 (4): 328–343.

33. Gorden BH, Kim JH, Sarver AL, Frantz AM, Breen M, Lindblad-Toh K, et al. Identification of three molecular and functional subtypes in canine hemangiosarcoma through gene expression profiling and progenitor cell characterization. Am J Pathol. 2014; 184: 985–995. https://doi.org/10.1016/j.ajpath.2013.12.025 PMID: 24525151

34. Kiupel M, Webster JD, Bailey KL, Best S, DeLay J, Detrisac CJ, et al. Proposal of a 2-tier histologic grading system for canine cutaneous mast cell tumors to more accurately predict biological behavior. Vet Pathol. 2011; 48: 147–155. https://doi.org/10.1177/0300985810386469 PMID: 21062911

35. Strefezzi RDF, Kleeb SR, Xavier JG, Dias JLC. Avaliação da proliferação celular como indicador prognóstico para mastocitomas cutâneos caninos. Pesqui Vet Bras. 2010; 30: 559–565.

36. Li H, Handsaker B, Wysoker A, Fennell T, Ruan J, Homer N, Abecasis G, Durbin R. The sequence alignment/map format and SAMtools. Bioinformatics. 2009; 25(16): 2078–2079. https://doi.org/10.1093/bioinformatics/btp352 PMID: 19505943

37. Anders S, Pyl PT, Huber W. HTSeq—a Python framework to work with high-throughput sequencing data. Bioinformatics. 2015; 31(2): 166–169. https://doi.org/10.1093/bioinformatics/btu638 PMID: 25260700

38. Robinson MD, McCarthy DJ, Smyth GK. edgeR: A Bioconductor package for differential expression analysis of digital gene expression data. Bioinformatics. 2009; 26: 139–140. https://doi.org/10.1093/bioinformatics/btp616 PMID: 19910308

39. Langfelder P, Horvath S. WGCNA: an R package for weighted correlation network analysis. BMC bioinformatics. 2008; 9: 559. https://doi.org/10.1186/1471-2105-9-559 PMID: 19114008

40. Zhang B, Horvath S. A general framework for weighted gene co-expression network analysis. Stat Appl Genet Mol Biol. 2005; 4(1).

41. Langfelder P., Zhang B., & Horvath S. Defining clusters from a hierarchical cluster tree: the Dynamic Tree Cut package for R. Bioinformatics. 2007; 24(5): 719–720. https://doi.org/10.1093/bioinformatics/btm563 PMID: 18024473

42. Patnaik AK, Ehler WJ, MacEwen EG. Canine cutaneous mast cell tumor: morphologic grading and survival time in 83 dogs. Vet Pathol. 1984; 21: 469–474. https://doi.org/10.1177/030098588402100503 PMID: 6435301

43. Subramanian A, Tamayo P, Mootha VK, Mukherjee S, Ebert BL, Gillette MA, Paulovich A, Pomeroy SL, Golub TR, Lander ES, Mesirov JP. Gene set enrichment analysis: a knowledge-based approach for interpreting genome-wide expression profiles. Proc Natl Acad Sci USA. 2005; 102(43): 15545–15550. https://doi.org/10.1073/pnas.0506580102 PMID: 16199517

44. Abadie JJ, Amardeilh MA, Delverdier ME. Immunohistochemical detection of proliferating cell nuclear antigen and Ki-67 in mast cell tumors from dogs. J Am Vet Med Assoc. 1999; 215: 1629–1634. PMID: 14567425

45. Scase TJ, Edwards D, Miller J, Henley W, Smith K, Blunden A, et al. Canine mast cell tumors: correlation of apoptosis and proliferation markers with prognosis. J Vet Intern Med. 2006; 20: 151–158. https://doi.org/10.1892/0891-6640(2006)20[151:cmctco]2.0.co;2 PMID: 16496935

46. Webster JD, Yuzbasiyan-Gurkan V, Miller RA, Kaneene JB, Kiupel M. Cellular proliferation in canine cutaneous mast cell tumors: associations with c-KIT and its role in prognostication. Vet Pathol. 2007; 44: 298–308. https://doi.org/10.1354/vp.44-3-298 PMID: 17491070

47. Dvorak HF. Tumors: wounds that do not heal. Similarities between tumor stroma generation and wound healing. New England Journal of Medicine. 1986; 315: 1650–1659. https://doi.org/10.1056/NEJM198612253152606 PMID: 3537791

48. Alberts J, Johnson B, Lewis A et al. The Extracellular Matrix of Animals. In: Alberts B, Johnson A, Lewis J, Raff M, Roberts K, Walter P, editors. Molecular Biology of the Cell 4th edition. New York: Garland Science; 2002. Available from: https://www.ncbi.nlm.nih.gov/books/NBK26810/

49. Schultz GS, Wysocki A. Interactions between extracellular matrix and growth factors in wound healing. Wound Repair Regen. 2009; 17: 153–162. https://doi.org/10.1111/j.1524-475X.2009.00466.x PMID: 19320882

50. Kagan HM, Li W. Lysyl oxidase: properties, specificity, and biological roles inside and outside of the cell. J Cell Biochem. 2003; 88: 660–672. https://doi.org/10.1002/jcb.10413 PMID: 12577300

51. Erler JT, Bennewith KL, Nicolau M, Dornhöfer N, Kong C, Le QT, Chi JT, Jeffrey SS, Giaccia AJ. Lysyl oxidase is essential for hypoxia-induced metastasis. Nature. 2006; 440: 1222–1226. https://doi.org/10.1038/nature04695 PMID: 16642001

52. Kirschmann DA, Seftor EA, Fong SF, Nieva DRC, Sullivan CM, Edwards EM, Sommer P, Csiszar K, Hendrix MJC. A molecular role for lysyl oxidase in breast cancer invasion. Cancer Research. 2002; 62: 4478–4483. PMID: 12154058

53. Akiri G, Sabo E, Dafni H, Vadasz Z, Kartvelishvily Y, Gan N, Kessler O, Cohen T, Resnick M, Neeman M, Neufeld G. Lysyl oxidase-related protein-1 promotes tumor fibrosis and tumor progression in vivo. Cancer Research. 2003; 63: 1657–1666. PMID: 12670920

54. Hollosi P, Yakushiji JK, Fong KS, Csiszar K, Fong SF. Lysyl oxidase–like 2 promotes migration in noninvasive breast cancer cells but not in normal breast epithelial cells. Int J Cancer. 2009; 125: 318–327. https://doi.org/10.1002/ijc.24308 PMID: 19330836

55. Peng L, Ran YL, Hu H, Yu L, Liu Q, Zhou Z, Sun YM, Sun LC, Pan J, Sun LX, Zhao P, Yang ZH. Secreted LOXL2 is a novel therapeutic target that promotes gastric cancer metastasis via the Src/FAK pathway. Carcinogenesis. 2009; 30: 1660–1669. https://doi.org/10.1093/carcin/bgp178 PMID: 19625348

56. Erez N, Truitt M, Olson P, Hanahan D. Cancer-associated fibroblasts are activated in incipient neoplasia to orchestrate tumor-promoting inflammation in an NF-κB-dependent manner. Cancer cell. 2010; 17: 135–147. https://doi.org/10.1016/j.ccr.2009.12.041 PMID: 20138012

57. Micke P, Ostman A. Tumour-stroma interaction: cancer-associated fibroblasts as novel targets in anti-cancer therapy? Lung cancer. 2004; 45 Suppl: 163–175.

58. Kalluri R, Zeisberg M. Fibroblasts in cancer. Nat Rev Cancer. 2006; 6: 392–401. https://doi.org/10.1038/nrc1877 PMID: 16572188

59. Schor SL, Schor AM, Grey AM, Rushton G. Foetal and cancer patient fibroblasts produce an autocrine migration-stimulating factor not made by normal adult cells. J Cell Sci.1998; 90: 391–399.

60. Durning P, Schor SL, Sellwood RA. Fibroblasts from patients with breast cancer show abnormal migratory behaviour in vitro. The Lancet. 1984; 324: 890–892.

61. Mueller MM, Fusenig NE. Friends or foes—bipolar effects of the tumour stroma in cancer. Nature Rev Cancer. 2004; 4: 839–849.

62. Tsukada T, McNutt MA, Ross R, Gown AM. HHF35, a muscle actin-specific monoclonal antibody II. Reactivity in normal, reactive, and neoplastic human tissues. Am J Pathol. 1987; 127: 389–402. PMID: 3555106

63. Ronnov-Jessen L, Petersen OW, Bissell MJ. Cellular changes involved in conversion of normal to malignant breast: importance of the stromal reaction. Physiol Rev. 1996; 76: 69–125. https://doi.org/10.1152/physrev.1996.76.1.69 PMID: 8592733

64. Gabbiani G. The myofibroblast in wound healing and fibrocontractive diseases. J Pathol. 2003; 200: 500–503. https://doi.org/10.1002/path.1427 PMID: 12845617

65. Allinen M, Beroukhim R, Cai L, Brennan C, Lahti-Domenici J, Huang H, Porter D, Hu M, Chin L, Richardson A, Schnitt S, Sellers WR, Polyak K. Molecular characterization of the tumor microenvironment in breast cancer. Cancer Cell. 2004; 6: 17–32. https://doi.org/10.1016/j.ccr.2004.06.010 PMID: 15261139

66. Bhowmick NA, Neilson EG, Moses HL. Stromal fibroblasts in cancer initiation and progression. Nature. 2004; 432: 332–337. https://doi.org/10.1038/nature03096 PMID: 15549095

67. Orimo A, Gupta PB, Sgroi DC, Arenzana-Seisdedos F, Delaunay T, Naeem R, Carey VJ, Richardson AL, Weinberg RA. Stromal fibroblasts present in invasive human breast carcinomas promote tumor growth and angiogenesis through elevated SDF-1/CXCL12 secretion. Cell. 2005; 121: 335–348. https://doi.org/10.1016/j.cell.2005.02.034 PMID: 15882617

68. Tsujino T, Seshimo I, Yamamoto H, Ngan CY, Ezumi K, Takemasa I, Ikeda M, Sekimoto M, Matsuura N, Monden M. Stromal myofibroblasts predict disease recurrence for colorectal cancer. Clin Cancer Res 2007; 13(7): 2082–2090. https://doi.org/10.1158/1078-0432.CCR-06-2191 PMID: 17404090

69. Erkan M, Michalski CW, Rieder S, Reiser-Erkan C, Abiatari I, Kolb A,. Giese NA, Esposito I, Friess H, Kleef J. The activated stroma index is a novel and independent prognostic marker in pancreatic ductal adenocarcinoma. Clin Gastroenterol Hepatol. 2008; 6: 1155–1561. https://doi.org/10.1016/j.cgh.2008.05.006 PMID: 18639493

70. Yamashita M, Ogawa T, Zhang X, Hanamura N, Kashikura Y, Takamura M, Yoneda M, Shiraishi T. Role of stromal myofibroblasts in invasive breast cancer: stromal expression of alpha-smooth muscle actin correlates with worse clinical outcome. Breast Cancer. 2012; 19: 170–176. https://doi.org/10.1007/s12282-010-0234-5 PMID: 20978953

71. Klobukowska HJ, Munday JS. High Numbers of Stromal Cancer-Associated Fibroblasts Are Associated With a Shorter Survival Time in Cats With Oral Squamous Cell Carcinoma. Vet Pathol. 2016; 53: 1124–1130. https://doi.org/10.1177/0300985816629713 PMID: 26940838

72. Barry-Hamilton V., Spangler R., Marshall D., McCauley S., Rodriguez H. M., Oyasu M., et al. Allosteric inhibition of lysyl oxidase-like-2 impedes the development of a pathologic microenvironment. Nature medicine. 2010; 16: 1009–1017. https://doi.org/10.1038/nm.2208 PMID: 20818376